



# Flexible low-voltage organic phototransistors based on air-stable dinaphtho[2,3-b:2',3'-f]thieno[3,2-b]thiophene (DNNT)



Johannes Milvich<sup>a,\*</sup>, Tarek Zaki<sup>a</sup>, Mahdieh Aghamohammadi<sup>b</sup>, Reinhold Rödel<sup>b</sup>, Ulrike Kraft<sup>b</sup>, Hagen Klauk<sup>b</sup>, Joachim N. Burghartz<sup>a</sup>

<sup>a</sup>Institute for Microelectronics Stuttgart (IMS CHIPS), 70569 Stuttgart, Germany

<sup>b</sup>Max Planck Institute for Solid State Research, 70569 Stuttgart, Germany

## ARTICLE INFO

### Article history:

Received 13 October 2014

Received in revised form 2 February 2015

Accepted 4 February 2015

Available online 11 February 2015

### Keywords:

Dinaphthothienothiophene (DNNT)

Organic phototransistor

Optical characterization

Optical sensor

Threshold voltage shift

Dielectric interface trapping

## ABSTRACT

Photosensitive elements based on organic thin-film transistors readily integrated into flexible, large-area organic circuits open up new scopes in light-sensing applications. In this work, high-performance, low-voltage organic thin-film transistors based on dinaphtho[2,3-b:2',3'-f]thieno[3,2-b]thiophene (DNNT) are thoroughly characterized with respect to their optical functionality. The fundamental light-dependent effect, i.e., a large but slow threshold-voltage shift based on charge trapping in the aluminum oxide of the gate dielectric or at the semiconductor–dielectric interface, is analyzed depending on various parameters, such as biasing conditions, integration time, wavelength and power of the incoming light as well as the channel length. An optimized 3-phase operation consisting of reset, integration and read-out is proposed in order to maximize reproducibility, sensitivity and responsivity of the phototransistors. Two distinct regimes, an absorption-limited and a trapping-limited regime, are identified depending on the density of available trappable electrons, which is determined by the optical input power and the integration time. The maximum operation frequency is found to be larger in phototransistors with shorter channel lengths. Based on these results, an organic gesture recognition system with a refresh rate of 1 Hz was designed, implemented and successfully tested.

© 2015 Elsevier B.V. All rights reserved.

## 1. Introduction

Organic thin-film transistors (OTFTs) and circuits pose a promising way of manufacturing electronic systems with new properties, as they can be fabricated on flexible, large-area substrates [1,2]. Applications range from organic active-matrix displays [3] and adaptive lighting panels to medical applications [4], wearable devices [5] or packaging [6]. Many of these applications require some sort of sensor, capable of extracting data from the environment, such as pressure, temperature, humidity or light. Imaging capabilities could potentially have the widest range of applications, as they can be used for example for photography, scanning,

object or movement detection or range finding. Due to the high spatial resolution of typical image sensors, the required control and read-out logic tends to be sophisticated. Rigid image sensors have made a lot of progress in the past decades, and the majority of mobile consumer devices, such as smartphones and tablets, contain at least one of them. A flexible and printable version would be desirable and open up even more possible applications. Gesture or motion based interactions between humans and almost any surface or large-area scanning of objects are just some of the prospects. In 2005, Someya et al. demonstrated a flexible image sensor on a plastic substrate using organic photodiodes [7]. The fabrication process of organic imagers could, however, be simplified if efficient organic phototransistors (OPT) replaced the photodiodes. In the best case, these phototransistors are fabricated in exactly the same way as the logic

\* Corresponding author.

E-mail address: [milvich@ims-chips.de](mailto:milvich@ims-chips.de) (J. Milvich).

transistors surrounding them without adding a substantial number of extra process steps. This would lead to an easy-to-integrate optical and electrical circuit on a common flexible substrate. This work aims to use existing, high-performance OTFTs [8] as photo-sensing elements, i.e., as OPTs, and poses the question if they are viable for a sensor application. In order to answer this question, the effect of illumination on the OTFTs has to be studied thoroughly. Furthermore, proper biasing sequences and read-out techniques have to be developed, which distinguish these opto-electric transducers from memory-type organic transistors [9,10]. OPTs with various geometries and materials have already been investigated by other research groups within the past years [11–16,10]. However, the low-voltage operation of 2–3 V and the large effective mobility greater than  $1.2 \text{ cm}^2/\text{Vs}$  at channel lengths as short as  $1 \mu\text{m}$  demonstrated in [8] encourage further investigation.

## 2. Methods and materials

### 2.1. Fabrication

All transistors and phototransistors were fabricated in the inverted-staggered (bottom-gate, top-contact) configuration on a flexible polyethylene naphthalate (PEN) substrate using a set of 4 high-resolution silicon stencil masks [17]. First, a thin layer of gold (Au) was deposited by thermal evaporation in vacuum and patterned through a first stencil mask to define the routing (interconnect) layer. In the second step, aluminum (Al) was vacuum-deposited through a second mask to define the gate electrodes of all transistors. Next, the hybrid gate dielectric consisting of a 3.6 nm thick layer of oxygen-plasma-grown aluminum oxide ( $\text{AlO}_x$ ) and a 1.7 nm thick self-assembled monolayer (SAM) of n-tetradecylphosphonic acid was formed. The small thickness (5.3 nm) and large capacitance ( $600 \text{ nF}/\text{cm}^2$ ) of the  $\text{AlO}_x$ /SAM gate dielectric enable low-voltage operation of the transistors. Despite the small dielectric thickness, the undesirable leakage currents are negligibly small [8]. A 25-nm-thick layer of the high-mobility organic semiconductor DNNT [18] was then sublimated through a third stencil mask. Finally, Au source/drain contacts were patterned using a fourth mask,

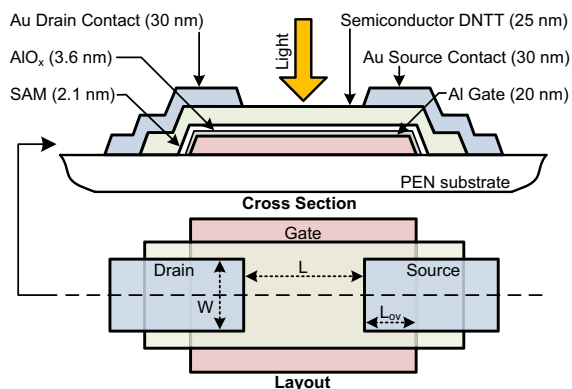


**Fig. 1.** Cross section and layout of a top-illuminated, inverted-staggered (bottom-gate, top-contact) organic phototransistor.

defining a channel length  $L$  of 4–100  $\mu\text{m}$  and a gate-to-contact overlap  $L_{ov}$  of 10  $\mu\text{m}$ . The schematic cross section and layout can be seen in Fig. 1. The transistors are illuminated from the top, as the gate metal is opaque. Therefore, light mainly enters the device in the intrinsic transistor area.

### 2.2. Measurement setup

A controlled illumination environment and measurement setup was established. A 250 W Schott KL2500 cold light source and a color filter wheel with a typical filter bandwidth of 10 nm is used to create light with a wavelength between 200 and 1100 nm. Subsequently, an integrating sphere with a built-in reference detector generates a homogeneous, well-defined light field. The gate, drain and source contacts of the transistors are connected to a two-channel Keithley 2636A System Source Meter Instrument. This setup can perform automated spectral analysis of the transistors' direct current (DC) properties within a controlled, adjustable illumination environment. The optical absorption properties of the organic semiconductor DNNT are determined by a transmission measurement. This experiment was performed using a glass substrate with a stack of  $\text{AlO}_x$  (by atomic layer deposition), a SAM and DNNT, and the measured spectrum was referenced against that obtained from a substrate without DNNT. The measured spectrum indicates sensitivity to ultraviolet (UV) and blue illumination (see Fig. 2).

## 3. Results and discussion

### 3.1. Light-induced threshold voltage shift

Under illumination, the p-channel DNNT OPTs show a strong and slow threshold-voltage shift  $\Delta V_{th}$  towards more positive values, which is attributed to the formation of an additional charge sheet caused by the trapping of photo-generated electrons. The trap centers are believed to be located either in the bulk of the  $\text{AlO}_x$  (which the electrons can reach by tunneling through the 1.7 nm thick SAM) or

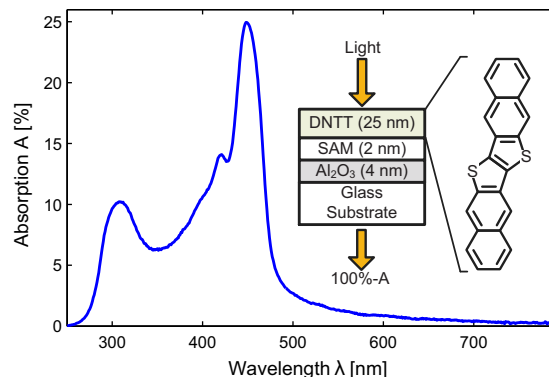


**Fig. 2.** UV/Vis absorption spectrum of a 25 nm thick film of the organic semiconductor DNNT deposited onto a stack of  $\text{AlO}_x$  (deposited by atomic layer deposition) and a tetradecylphosphonic acid SAM on a glass substrate. The absorption of a reference substrate without DNNT has been subtracted. Inset: Schematic cross-section of the substrate employed for the absorption measurement, and molecular structure of DNNT.

at the interface between the semiconductor and the SAM (perhaps at grain boundaries or other structural defects). Although freshly grown  $\text{AlO}_x$  surfaces have a large density of hydroxyl groups that could potentially act as electron traps, these hydroxyl groups are eliminated during the grafting of the alkylphosphonic acid SAM [19] and are thus unlikely to play a role here, while trapping in the bulk of the semiconductor can be ruled out because it would produce a different response in the channel modulation. In dark conditions, only a negligible  $\Delta V_{\text{th}}$  is observed, the reason being that only few minority charge carriers, i.e., free electrons, are injected into the semiconductor because of the large energy barrier between the Fermi level of the contact metal (Au) and the lowest unoccupied molecular orbital (LUMO) of DNTT, even at a large drain-source voltage  $V_{\text{DS}}$ . If light with photon energies within the absorption range of the organic semiconductor enters the device, electron-hole pairs are created. Dissociation, which can be enhanced with an electrical field, creates additional electrons and holes, possibly increasing the trap rate and thus the  $V_{\text{th}}$  shift.

In order to achieve reproducible results from subsequent measurements, the devices have to be reset before each measurement. This is done by creating an accumulation channel with a large negative gate-source voltage  $V_{\text{GS}}$  while applying a small  $V_{\text{DS}}$  in order to release trapped charges from the dielectric interface. The reset process can take several seconds to minutes, depending on the initial  $V_{\text{th}}$  displacement caused by illumination or excessive bias stress.

### 3.2. Parameter dependencies

This section discusses how the light-induced  $\Delta V_{\text{th}}$  is affected by various parameters, such as biasing conditions, integration time, wavelength and power of the incoming light, and the channel length of the transistor. During illumination,  $V_{\text{GS}}$  has a large impact on  $\Delta V_{\text{th}}$ , as it can attract electrons to or repel them from the dielectric interface. A large positive  $V_{\text{GS}}$  during illumination (for a certain

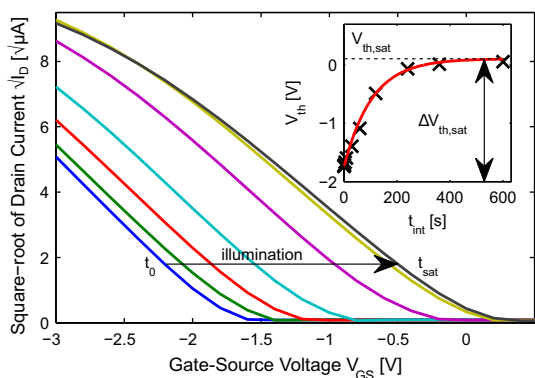


**Fig. 3.** Light-induced threshold-voltage shift in an organic phototransistor ( $L = 10 \mu\text{m}$ ,  $W = 1000 \mu\text{m}$ ). Each of the transfer curves was measured at  $V_{\text{DS}} = -1.5 \text{ V}$  after a certain integration time  $t_{\text{int}}$  under illumination ( $\lambda = 461 \text{ nm}$ ,  $P_{\text{opt}} = 66 \text{ nW}$ ,  $V_{\text{GS}} = +3 \text{ V}$ ,  $V_{\text{DS}} = 0 \text{ V}$ ). After each measurement, a reset phase was applied ( $V_{\text{GS}} = -3 \text{ V}$ ,  $V_{\text{DS}} = -0.1 \text{ V}$ ) that recovers the original  $V_{\text{th}}$ . Inset: The exponential dependence of  $V_{\text{th}}$  on  $t_{\text{int}}$  indicates that the process is trap-related. The threshold-voltage shift eventually saturates.

integration time  $t_{\text{int}}$ ) produces the fastest positive  $\Delta V_{\text{th}}$ , whereas a large negative  $V_{\text{GS}}$  helps with returning the device to the initial state. It has to be noted that during illumination with a large positive  $V_{\text{GS}}$ , no  $V_{\text{DS}}$  should be applied to achieve a homogeneous field distribution and trapping throughout the channel, whereas during reset, a small  $V_{\text{DS}}$  helps with supplying holes for recombination with the released electrons. Fig. 3 shows how the transfer characteristics of a DNTT OPT (channel length  $L = 10 \mu\text{m}$ , width  $W = 1000 \mu\text{m}$ ) shift as a result of illumination for various integration times from 0 to 360 s. During integration,  $V_{\text{GS}}$  and  $V_{\text{DS}}$  are held constant at +3 V and 0 V, and the transistor is illuminated with light having a wavelength of  $\lambda = 461 \text{ nm}$  and an optical power of  $P_{\text{opt}} = 66 \text{ nW}$ . During read-out,  $V_{\text{DS}}$  is set to  $-1.5 \text{ V}$ . The threshold voltage shifts by approximately 2 V from the initial state in the dark at  $t_0$  before saturating after a time  $t_{\text{sat}}$ . The  $V_{\text{th}}$  extracted after various integration times is shown in the inset in Fig. 3. An exponential fit can be applied according to the following equation:

$$V_{\text{th}}(t_{\text{int}}) = \Delta V_{\text{th,sat}} \exp\left(-\frac{t_{\text{int}}}{\tau}\right) + V_{\text{th,sat}} \quad (1)$$

Here,  $V_{\text{th}}$  is expressed by means of  $\Delta V_{\text{th,sat}}$ , which is the total  $\Delta V_{\text{th}}$  from device reset to an equilibrium state under illumination,  $V_{\text{th,sat}}$ . Eq. (1) is often used to describe trap-related processes and shows that for large integration times and a strong illumination, i.e., when many trappable electrons are present, the process is truly trapping limited [14]. From the exponential fit, a time constant of  $\tau = 115 \text{ s}$  is extracted. The characteristically long response time of this trap-related process is partly responsible for the fact that phototransistors are inferior to photodiodes as fast-response optical sensors. However, unlike photodiodes, which often require external amplification, phototransistors have a built-in amplification given by their transconductance  $g_m$ . Thus, a useful signal shift is already achieved after integration times much shorter than  $t_{\text{sat}}$ , as there is no need to wait for complete saturation of  $V_{\text{th}}$ .

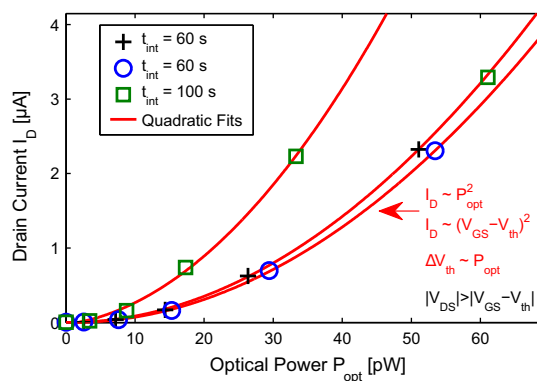


**Fig. 4.** The drain current measured in the transistor's saturation regime ( $L = 4 \mu\text{m}$ ,  $W = 200 \mu\text{m}$ ,  $V_{\text{GS}} = V_{\text{DS}} = -2 \text{ V}$ ) after various integration times  $t_{\text{int}}$  under illumination ( $\lambda = 461 \text{ nm}$ ) scales quadratically with the optical power  $P_{\text{opt}}$  when  $P_{\text{opt}}$  is small and  $t_{\text{int}}$  is short compared with  $t_{\text{sat}}$ . The resulting linear relationship between  $V_{\text{th}}$  and  $P_{\text{opt}}$  indicates that the process is absorption-limited. In contrast, the process is trapping-limited when  $P_{\text{opt}}$  is large (e.g., 60 pW) and  $t_{\text{int}}$  is long (e.g., 100 s).

The light-induced threshold voltage shift is not always trapping limited, however. For smaller  $P_{\text{opt}}$  and for shorter  $t_{\text{int}}$ ,  $\Delta V_{\text{th}}$  is in fact limited by optical absorption. Fig. 4 plots the drain current  $I_D$  versus  $P_{\text{opt}}$  in the transistor's saturation regime. When the product of  $P_{\text{opt}}$  and  $t_{\text{int}}$  is sufficiently small, the relationship is well-described by a quadratic fit. Within this region,  $\Delta V_{\text{th}}$  increases linearly with  $P_{\text{opt}}$  due to the additional amount of photo-generated charges per unit area trapped in the  $\text{AlO}_x$  or at the semiconductor-dielectric interface,  $Q_f$ :

$$\Delta V_{\text{th}} = \frac{Q_f}{C_I} + V_{\text{inj}} \propto P_{\text{opt}}. \quad (2)$$

Here,  $C_I$  is the gate-dielectric capacitance per unit area and  $V_{\text{inj}}$  is a contribution from the contact resistance [20]. The influence of  $V_{\text{inj}}$  on  $\Delta V_{\text{th}}$  is neglected here, as  $\Delta V_{\text{th}}$  shows no dependency on  $V_{\text{DS}}$ . When  $P_{\text{opt}}$  and  $t_{\text{int}}$  are large ( $\geq 60$  pW,  $\geq 100$  s), the relationship between  $\Delta V_{\text{th}}$  and  $P_{\text{opt}}$  is no longer linear, indicating a transition from the absorption-limited process to the previously mentioned trapping-limited process. The trap density is estimated with  $\Delta V_{\text{th,sat}} = 2$  V and  $C_I = 600$  nF/cm<sup>2</sup> as  $Q_f \approx 10^{13}$  1/cm<sup>2</sup>.

The spectral sensitivity  $I_{\text{on}}/I_{\text{off}}$  of the device matches the measured absorption spectrum of the organic semiconductor (shown in Fig. 2). Regardless of the wavelength, the maximum sensitivity is achieved if  $V_{\text{GS}}$  applied during read-out equals  $V_{\text{GS}}$  at the lower end of the subthreshold regime in dark conditions,  $V_{\text{on,dark}}$ . This is due to the steep, exponential current increase in the subthreshold regime. The highest responsivity  $R = I_{\text{on}}/P_{\text{opt}}$  is obtained at  $|V_{\text{DS}} - V_{\text{th}}| > |V_{\text{GS}}| > |V_{\text{th,dark}}|$ , as the absolute current change is much larger above than below  $V_{\text{th}}$ , and larger in saturation than in the linear regime. In a transistor with  $L = 10$   $\mu\text{m}$  and  $W = 1000$   $\mu\text{m}$ , under illumination at  $\lambda = 460$  nm and  $P_{\text{opt}} = 66$  nW, the sensitivity and responsivity peaked at  $I_{\text{on}}/I_{\text{off}} = 10^9$  and  $R = 10^5$  A/W,

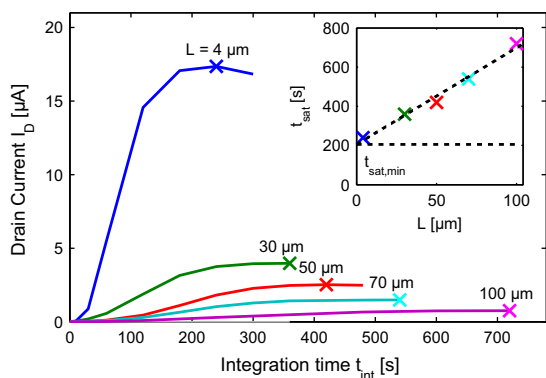


**Fig. 5.** The drain current measured after various times under illumination saturates faster in transistors with shorter channel lengths  $L$  ( $W = 200$   $\mu\text{m}$ ). Inset: The time it takes for the light-induced threshold-voltage shift to saturate is proportional to  $L$ . It has a lower limit  $t_0$  related to the mean trapping time of electrons. The fact that  $t_{\text{sat}}$  scales with  $L$  can be explained by the greater probability that electrons recombine with holes that are less quickly removed from the semiconductor following exciton dissociation when  $L$  is large.

respectively. These large values are, however, only achieved if  $V_{\text{th}}$  is allowed to saturate after approximately 5 min of illumination.

The geometry of the device, especially the active area  $A = W \times L$ , does not have an impact on the total  $\Delta V_{\text{th,sat}}$ . Measurements on OPTs with various dimensions show that  $\Delta V_{\text{th,sat}}$  is independent of the channel length, which is in agreement with (2), as  $\Delta V_{\text{th,sat}}$  depends only on the density of traps per unit area  $Q_f$ . Since the absolute threshold-voltage shift is independent of the transistor's active area, OPTs can be scaled down without losing sensitivity, contrary to photodiodes [21]. In contrast to  $\Delta V_{\text{th,sat}}$ ,  $t_{\text{sat}}$  does in fact depend on the channel length. Fig. 5 shows that in transistors with shorter channel lengths, the saturated state is reached faster. The inset plots the extracted  $t_{\text{sat}}$  versus  $L$ , indicating two interesting properties. The first observation is that  $t_{\text{sat}}$  scales linearly with  $L$ . This can be explained as follows: The rate at which the threshold voltage shifts under illumination is determined by the rate at which electrons are trapped. In short-channel OPTs, excess holes are quickly removed from the semiconductor through the nearby contacts after exciton dissociation, so that the probability that an electron recombines with a hole before being trapped is small. In long-channel devices, the electron-trapping rate is reduced by the greater probability that electrons recombine with excess holes before being trapped. The second observation is the existence of a lower limit  $t_{\text{sat,min}}$ . This can be attributed to the average trapping time of a free electron present at the interface.

### 3.3. Gesture recognition system

Based on the results described in the previous sections, the light-induced threshold-voltage shift in OPTs can be optimized. To demonstrate this, we have designed and implemented an array of 16 OPTs covering an area of  $2 \times 4$  cm<sup>2</sup> on a flexible PEN substrate. An optimized 3-phase operation is implemented, consisting of a reset

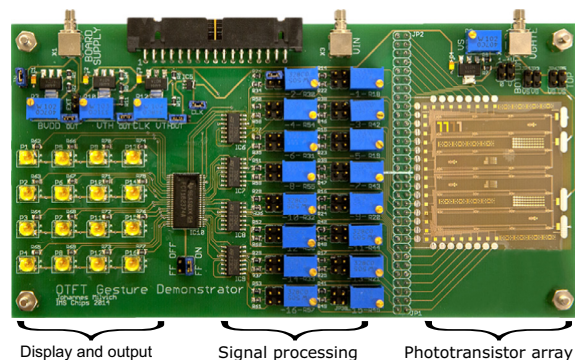


**Fig. 6.** Gesture recognition system with two arrays of 16 organic phototransistors on a flexible plastic substrate, glued onto a circuit board for testing. A 3-phase reset/integrate/read-out protocol optimizes the light-induced threshold-voltage shift in the transistors. The threshold-voltage shift produces a modulation of the drain current that is used to translate the spatial illumination information across the photosensor array into electrical signals, displayed live in a  $4 \times 4$  LED array and available for external read-out.

phase ( $V_{GS} = -3\text{ V}$ ,  $V_{DS} = -0.1\text{ V}$ ) to achieve reproducible results by resetting  $V_{th}$  to an initial state, an integration phase ( $V_{GS} = +3\text{ V}$ ,  $V_{DS} = 0\text{ V}$ ) to enhance the trapping rate and thus  $\Delta V_{th}/\Delta t$ , and a read-out phase ( $V_{GS} = V_{th,dark}$ ,  $V_{DS} = V_{th,dark}$ ) to optimize responsivity. This 3-phase operation maximizes the light-induced threshold-voltage shift while eliminating signal drift and thus provides a reproducible modulation of the drain current at a fixed bias condition that can be used to detect spatially resolved illumination information across the sensor array operated with a refresh rate of 1 Hz. The drain currents of all OPTs are translated into 1-bit information on a printed circuit board and are continuously displayed in an LED array for demonstration purposes (see Fig. 6). Alternatively, the sensor data can be read out externally for further processing.

#### 4. Conclusion

The effect of illumination on high-performance, low-voltage, DNTT-based OTFTs was thoroughly investigated. With proper biasing, the absorption of UV/blue light in the p-channel organic semiconductor DNTT leads to a significant increase in the density of free electrons, which can be trapped in the  $\text{AlO}_x$  of the gate dielectric or in the semiconductor, at grain boundaries or structural defects reaching the interface of the SAM. This produces a strong but slow threshold voltage shift that translates into a large current modulation through the internal amplification of the OTFT. Depending on the channel length of the transistors, the light-induced threshold-voltage shift saturates more or less rapidly, and its final value depends only on the density of trapped electrons. This means that phototransistors can be aggressively scaled down without losing sensitivity, which is an important advantage compared with photodiodes. In principle, it is found that the process is absorption limited for small optical powers and short integration times, while the process becomes trapping limited when the density of light-induced electrons exceeds a certain value. The measured parameter dependencies were used to implement an array of organic phototransistors on a flexible substrate that can perform gesture recognition at a refresh rate of 1 Hz. Future work could aim for a more complex circuit, where OPTs and regular OTFTs are fabricated on the same substrate. A selective shielding layer could decouple the regular OTFTs from the light-induced threshold voltage shift in the OPTs.

#### Acknowledgments

The authors gratefully acknowledge Prof. Kazuo Takimiya (Center for Emergent Matter Science, RIKEN, Wako, Saitama, Japan) for providing the organic semiconductor DNTT employed in this study, Harald Richter for his valuable input and Marion Hagel for wire-bonding of the flexible substrates. This work was partially funded by the German Ministry of Education and Research (BMBF) under Grant 1612000463 (KoSiF).

#### References

- [1] T. Someya, Y. Kato, T. Sekitani, S. Iba, Y. Noguchi, Y. Murase, H. Kawaguchi, T. Sakurai, Conformable, flexible, large-area networks of pressure and thermal sensors with organic transistor active matrixes, *Proc. Nat. Acad. Sci. USA* 102 (35) (2005) 12321–12325, <http://dx.doi.org/10.1073/pnas.0502392102>.
- [2] S.R. Forrest, The path to ubiquitous and low-cost organic electronic appliances on plastic, *Nature* 428 (6986) (2004) 911–918, <http://dx.doi.org/10.1038/nature02498>.
- [3] G.H. Gelinck, H.E.A. Huitema, E. van Veenendaal, E. Cantatore, L. Schrijnemakers, J.B. van der Putten, T.C. Geuns, M. Beenhakkers, J.B. Giesbers, B.-H. Huisman, et al., Flexible active-matrix displays and shift registers based on solution-processed organic transistors, *Nat. Mater.* 3 (2) (2004) 106–110, <http://dx.doi.org/10.1038/nmat1061>.
- [4] G.H. Gelinck, A. Kumar, D. Moet, J.-L. van der Steen, U. Shafiq, P.E. Malinowski, K. Myny, B.P. Rand, M. Simon, W. Rütten, et al., X-ray imager using solution processed organic transistor arrays and bulk heterojunction photodiodes on thin, flexible plastic substrate, *Org. Electron.* 14 (10) (2013) 2602–2609, <http://dx.doi.org/10.1016/j.orgel.2013.06.020>.
- [5] M. Barbaro, A. Caboni, P. Cosseddu, G. Mattana, A. Bonfiglio, Active devices based on organic semiconductors for wearable applications, *IEEE Trans. Inf Technol. Biomed.* 14 (3) (2010) 758–766, <http://dx.doi.org/10.1109/TITB.2010.2044798>.
- [6] V. Subramanian, J.M. Fréchet, P.C. Chang, D.C. Huang, J.B. Lee, S.E. Molesa, A.R. Murphy, D.R. Redinger, S.K. Volkman, Progress toward development of all-printed RFID tags: materials, processes, and devices, *Proc. IEEE* 93 (7) (2005) 1330–1338, <http://dx.doi.org/10.1109/JPROC.2005.850305>.
- [7] T. Someya, Y. Kato, S. Iba, Y. Noguchi, T. Sekitani, H. Kawaguchi, T. Sakurai, Integration of organic FETs with organic photodiodes for a large area, flexible, and lightweight sheet image scanners, *IEEE Trans. Electr. Dev.* 52 (11) (2005) 2502–2511, <http://dx.doi.org/10.1109/TED.2005.857935>.
- [8] U. Zschieschang, R. Hofmockel, R. Rödel, U. Kraft, M.J. Kang, K. Takimiya, T. Zaki, F. Letzkus, J. Butschke, H. Richter, et al., Megahertz operation of flexible low-voltage organic thin-film transistors, *Org. Electron.* 14 (6) (2013) 1516–1520, <http://dx.doi.org/10.1016/j.orgel.2013.03.021>.
- [9] M. Kang, K.-J. Baeg, D. Khim, Y.-Y. Noh, D.-Y. Kim, Printed, flexible, organic nano-floating-gate memory: effects of metal nanoparticles and blocking dielectrics on memory characteristics, *Adv. Funct. Mater.* 23 (28) (2013) 3503–3512, <http://dx.doi.org/10.1002/adfm.201203417>.
- [10] X. Ren, P.K. Chan, 23 bits optical sensor based on nonvolatile organic memory transistor, *Appl. Phys. Lett.* 104 (11) (2014) 113302, <http://dx.doi.org/10.1063/1.4869308>.
- [11] K. Narayan, N. Kumar, Light responsive polymer field-effect transistor, *Appl. Phys. Lett.* 79 (12) (2001) 1891–1893, <http://dx.doi.org/10.1063/1.1404131>.
- [12] M.C. Hamilton, S. Martin, J. Kanicki, Thin-film organic polymer phototransistors, *IEEE Trans. Electr. Dev.* 51 (6) (2004) 877–885, <http://dx.doi.org/10.1109/TED.2004.829619>.
- [13] Y.-Y. Noh, D.-Y. Kim, K. Yase, Highly sensitive thin-film organic phototransistors: effect of wavelength of light source on device performance, *J. Appl. Phys.* 98 (7) (2005) 074505, <http://dx.doi.org/10.1063/1.2061892>.
- [14] M. Debucquoy, S. Verlaak, S. Steudel, K. Myny, J. Genoe, P. Heremans, Correlation between bias stress instability and phototransistor operation of pentacene thin-film transistors, *Appl. Phys. Lett.* 91 (10) (2007), <http://dx.doi.org/10.1063/1.2777177>, 103508–103508.
- [15] S. Kim, T. Lim, K. Sim, H. Kim, Y. Choi, K. Park, S. Pyo, Light sensing in a photoresponsive, organic-based complementary inverter, *ACS Appl. Mater. Interfaces* 3 (5) (2011) 1451–1456, <http://dx.doi.org/10.1021/am101284m>.
- [16] J. Kim, S. Cho, Y.-H. Kim, S.K. Park, Highly-sensitive solution-processed 2, 8-difluoro-5, 11-bis (triethylsilyl)ethynyl anthradithiophene (dif-tesadt) phototransistors for optical sensing applications, *Org. Electron.* 15 (9) (2014) 2099–2106, <http://dx.doi.org/10.1016/j.orgel.2014.06.007>.
- [17] F. Letzkus, J. Butschke, B. Höflinger, M. Irmscher, C. Reuter, R. Springer, A. Ehrmann, J. Mathuni, Dry etch improvements in the SOI wafer flow process for IPL stencil mask fabrication, *Microelectr. Eng.* 53 (1) (2000) 609–612, [http://dx.doi.org/10.1016/S0167-9317\(00\)00388-9](http://dx.doi.org/10.1016/S0167-9317(00)00388-9).
- [18] T. Yamamoto, K. Takimiya, Facile synthesis of highly  $\pi$ -extended heteroarenes, dinaphtho [2, 3-b: 2', 3'-f] chalcogenopheno [3, 2-b] chalcogenophenes, and their application to field-effect transistors, *J.*

- Am. Chem. Soc. 129 (8) (2007) 2224–2225, <http://dx.doi.org/10.1021/ja068429z>.
- [19] P.J. Hotchkiss, S.C. Jones, S.A. Paniagua, A. Sharma, B. Kippelen, N.R. Armstrong, S.R. Marder, The modification of indium tin oxide with phosphonic acids: mechanism of binding, tuning of surface properties, and potential for use in organic electronic applications, *Acc. Chem. Res.* 45 (3) (2011) 337–346, <http://dx.doi.org/10.1021/ar200119g>.
- [20] F.S. Ante, Contact Effects in Organic Transistors, Ph.D. thesis, École Polytechnique Fédérale de Lausanne, 2011.
- [21] T. Lulé, S. Benthien, H. Keller, F. Mutze, P. Rieve, K. Seibel, M. Sommer, M. Bohm, Sensitivity of CMOS based imagers and scaling perspectives, *IEEE Trans. Electr. Dev.* 47 (11) (2000) 2110–2122, <http://dx.doi.org/10.1109/16.877173>.